

# **Polyaniline@MOF fiber derived Fe-Co oxide-based high performance electrocatalyst**

Qiqi Sha <sup>a</sup>, Jianrong Wang <sup>a</sup>, Yizhong Lu <sup>a</sup>, Zhenlu Zhao <sup>a,b\*</sup>

<sup>a</sup> *School of Material Science and Engineering, University of Jinan, Jinan 250022, Shandong, China.*

<sup>b</sup> *Department of Bionano Engineering, Hanyang University, Ansan 426-791, South Korea.*

† E-mail: mse\_zhaozl@ujn.edu.cn.

## **Material Synthesis and Characterization**

### **Material characterizations**

The microstructure and other microscopic information of the samples were characterised by SEM (Scanning Electron Microscopy, USA, FEI QUANTA FEG 250 field emission scanning electron microscope produced by FEI, secondary electron image resolution of 1.04 nm), TEM (Transmission Electron Microscope, LM1-125 produced by FEI, USA) and HAADF-STEM (High angle annular dark field scanning transmission electron microscopy, JEOL 2100F, JEOL, Japan). The element distribution and content of the microdomains in the samples were characterized by EDS (Energy Spectrometer, JEOL 2100F, JEOL, Japan). The lattice structure information of different temperature samples was characterized by XRD (X-ray diffraction, D8 Advance X-ray diffractometer manufactured by Bruker, Germany). The degree of order of the lattice structure of carbon in the sample was characterized using Raman (Raman spectral analysis, manufactured by HORIBA Scientific); the content and valence of different elements were characterized using XPS (X-ray photoelectron

spectroscopy, Thermo ESCALAB 250XI X-ray photoelectron spectroscopy analyser, Thermo Fisher Scientific, American); the specific surface area and pore size distribution of the sample were characterized using BET (The Brunauer–Emmett–Teller specific surface area, Pore Master-60 Fully Automatic Porosity Meter from Quantachrome Instruments).

## Chemicals

All chemicals are not specially treated and purified prior to use. Aniline (AR Shanghai Maclean Biochemical Technology Co., Ltd.). Ammonium persulfate (AR Tianjin Hengxing Chemical Reagent Manufacturing Co., Ltd.). HCl (AR Laiyang Fine Chemical Plant). 2,5-dihydroxyterephthalic acid (AR Shanghai Maclean Biochemical Technology Co., Ltd.).  $\text{FeCl}_2 \cdot 4\text{H}_2\text{O}$  (AR Tianjin Damao Chemical Reagent Factory).  $\text{Co}(\text{NO}_3)_2 \cdot 6\text{H}_2\text{O}$  (AR Shanghai Maclean Biochemical Technology Co., Ltd.). N, N-dimethylformamide (AR Tianjin Fuyu Fine Chemical Co., Ltd.). Anhydrous ethanol (AR Tianjin Fuyu Fine Chemical Co., Ltd.). Potassium hydroxide (AR Tianjin Hengxing Chemical Reagent Manufacturing Co., Ltd.). N-Methylpyrrolidone (AR Tianjin Damao Chemical Reagent Factory). Ammonia (AR Sinopharm Group Chemical Reagent Co., Ltd.). Deionized water (analytical grade, laboratory-made).

## Experimental Section

All electrochemical data were tested using CHI760E electrochemical workstation; the test for OER and capacitance performance was in 0.1 M KOH and 2 M KOH solution at room temperature, respectively; the tube furnace used in the pyrolysis process is OTF-1200X Tube furnace (Hefei Kejing Material Technology Co., Ltd.); the drying oven used for drying the precursor is (53L)-DZF- 6050 (Hefei Kejing Material Technology Co., Ltd.);

All potentials involved in this experiment were referenced to the reversible hydrogen electrode (RHE) calculated as  $E(\text{RHE}) = E(\text{Hg}(\text{l})|\text{Hg}_2\text{Cl}_2, \text{ saturated KCl solution}) + \text{pH} \cdot 0.059\text{V} + 0.241\text{V}$ . The potential of the  $E(\text{Hg}(\text{l})|\text{Hg}_2\text{Cl}_2, \text{ saturated KCl solution})$  reference electrode was 0.241V compared to RHE. The reference electrode was a saturated  $\text{Hg}(\text{l})|\text{Hg}_2\text{Cl}_2$  (Saturated KCl solution) electrode, the counter electrode is graphite electrode.

**Preparation of working electrode in OER performance test:** In the preparation of a standard OER working electrode, 5 mg of catalyst was added to 1 ml of absolute ethanol, shaken, and sonicated to make the catalyst uniformly

dispersed in the solvent. Then drop 20  $\mu$ l solution on the glassy carbon electrode (GC) and wait for it to dry to obtain a working electrode.

**Preparation of working electrode in supercapacitor performance test:**

First, prepare for the preparation of electrode materials. Cut the nickel foam into a rectangle of  $1 \times 1 \text{ cm}^2$ , first immerse it in a 6 M HCl aqueous solution, and soak in an ultrasonic bath for 10~15 minutes to remove the nickel oxide layer that may exist on the surface of the nickel foam. After that, ultrasonically clean the nickel foam with DI water and ethanol for 10~15 minutes and dry it in an oven at  $60 \text{ }^\circ\text{C}$  overnight. For powder materials, the slurry coating process is adopted: the calcined iron cobalt oxide/PANI nanofiber powder sample, acetylene black and polyvinylidene fluoride (PVDF) are put into a mortar with a mass ratio of 8:1:1, Add N-methylpyrrolidone (NMP) dropwise to it, grind for 10 to 20 minutes to make the material become a slurry, use a small paintbrush to brush on the foam nickel in an area of  $1 \times 1 \text{ cm}^2$ , and use a thin sheet to Scrape the material evenly and dry it in a vacuum at  $60 \text{ }^\circ\text{C}$ . Finally, the dried iron-cobalt oxide/PANI nanofiber/nickel foam flakes are pressurized to 10 MPa on a tablet press to obtain the required electrode sheet.

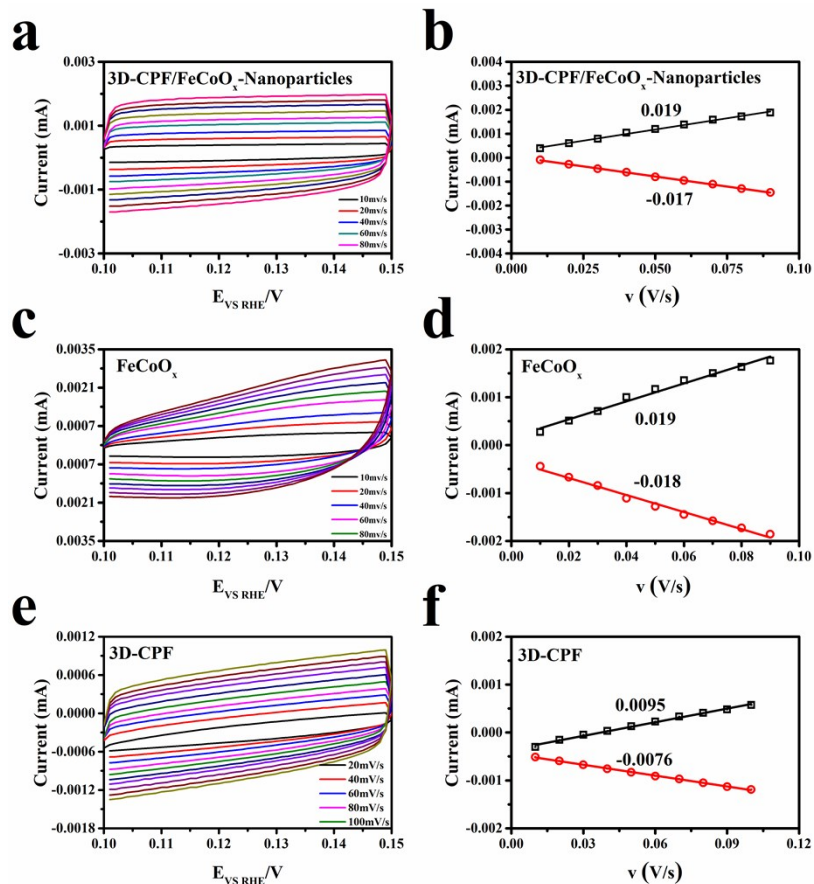


Figure S1: Double-layer capacitance measurements for determining electrochemically-active surface area from voltammetry. (a, c, e) CV curves of 3D-CPF/FeCoO<sub>x</sub>-Nanoparticles, FeCoO<sub>x</sub> and 3D-CPF at different scan rates. (b, d, f) The cathodic (red) and anodic (black) charging currents measured plotted as a function of scan rate of 3D-CPF/FeCoO<sub>x</sub>-Nanoparticles, FeCoO<sub>x</sub> and 3D-CPF.

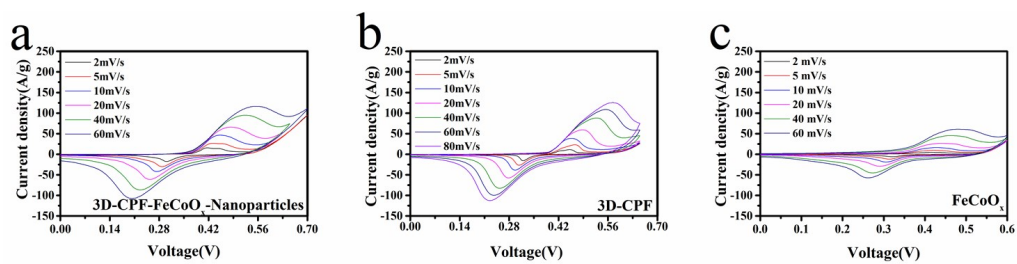


Figure S2: Cyclic voltammetry curve of 3D-CPF/FeCoO<sub>x</sub>-Nanoparticles, 3D-CPF and FeCoO<sub>x</sub>.

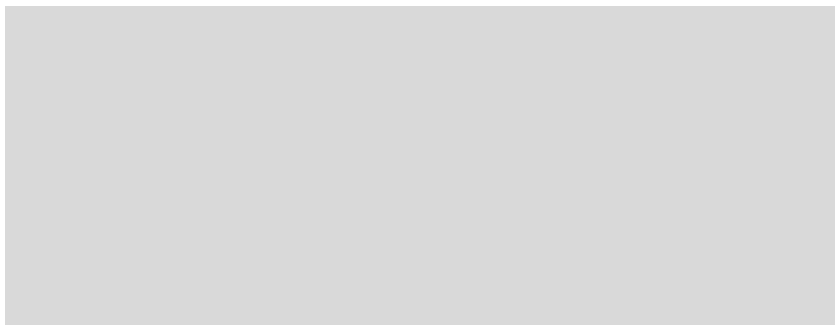


Figure S3: (a) Log ( $v$ ) versus log ( $i$ ) plot to verify the linearity of current on scan rate and for calculating  $b$  values. (b) Plot of  $v^{0.5}$  versus  $i \cdot v^{-0.5}$  for obtaining  $k_1$  and  $k_2$  values at various potentials in the cathodic sweep.

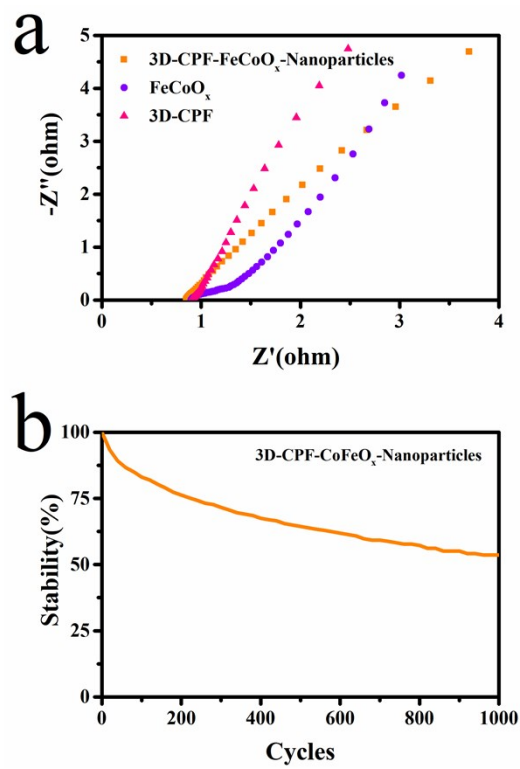


Figure S4: (a) Electrochemical Impedance Spectroscopy (EIS) curves 3D-CPF/FeCoO<sub>x</sub>-Nanoparticles, FeCoO<sub>x</sub> and 3D-CPF. (b) The stability curve of the material under the current density of 5 A/g for 1000 cycles of charge and discharge test of 3D-CPF/FeCoO<sub>x</sub>-Nanoparticles.

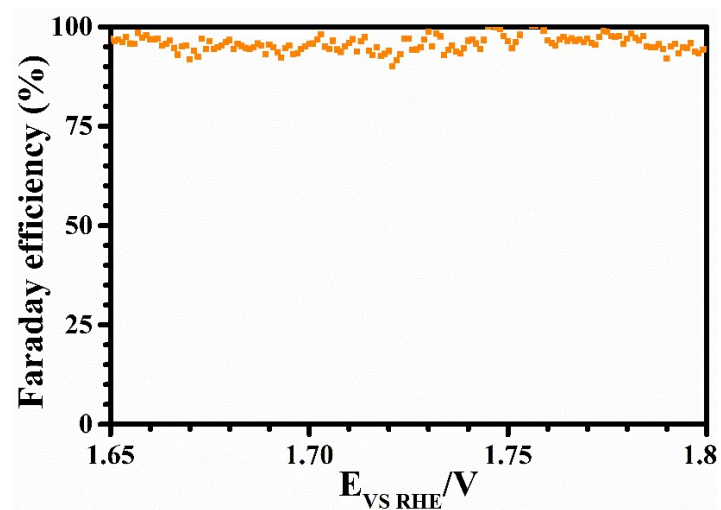


Figure S5: The Faraday efficiency of OER at different potentials during the 3D-CPF/FeCoO<sub>x</sub>-Nanoparticles catalysed OER reaction.